OFFICIAL USE ONLY / À USAGE EXCLUSIF

Design of porous architectures in laser powder bed fusion: effect of hatch spacing and rotation angle on density and pore morphology

Rene Lam[1], Tomisin Oluwajuyigbe[1], Sagar Patel[1], Mohsen K. Keshavarz[1], Mihaela Vlasea[1*]

[1] Multi-Scale Additive Manufacturing Laboratory, Department of Mechanical and Mechatronics Engineering, University of Waterloo, Waterloo, Ontario, N2G 4X8, Canada

* Corresponding author's email address: mihaela.vlasea@uwaterloo.ca

Abstract: Bone is a complex and hierarchical structure with the ability to provide extensive structural support to the body while also being lightweight for ease of motion. Bone can be damaged due to injury or illness, requiring the need for an orthopedic implant to enhance function, to provide structure and to encourage the growth of new bone. A challenge with current metal orthopedic implants is stress shielding, where there is a mismatch of mechanical moduli between the implant and human bone. When designing implants, it is important to tailor the mechanical response of the implant to natural bone to avoid stress shielding. This research explores a new method for implant design, incorporating pores stochastically using laser powder bed fusion (PBF-LB). This type of porosity is introduced into a solid metal part during printing by altering process parameters in PBF-LB. The density and pore morphology are dictated by the hatch spacing (100 – 500 µm) and rotation angle (60° and 67°). These structures were printed in Ti-6Al-4V. The effects of the hatch spacing and rotation angle on melt pool morphology and porosity were investigated, resulting in densities of 50.20 - 99.98% and columnar and stochastic pore morphologies.

Keywords: PBF-LB, Porous materials, Hatch spacing, Rotation angle, Low density

1. Introduction

Orthopedic implants are devices fabricated to replace bones and joints in the human body. They are required when the bones and joints in the body are injured, damaged, or fail to perform as needed [1]. As the need for orthopedic implants is gradually increasing due to the aging population, the need for better and optimized implants increases as well [2]. The functional requirements of orthopedic implants are to provide enough strength and stiffness to bear the load of the human body, be biocompatible with the body and promote bone healing and bone growth. Orthopedic implants manufactured with subtractive methods can meet these requirements as they are currently being used for replacement procedures, however they still have issues that lead to implant loosening and failure or require the need of revision surgeries. Implant loosening can be caused by an effect called stress shielding which is when the implant is too strong and stiff, which prevents bone growth in that region [3]. Porous materials like lattices or meshes can aid in reducing stress shielding in metallic implants by reducing its relative density and tailoring the mechanical response, however they are difficult to manufacture using conventional subtractive manufacturing methods. Additive manufacturing (AM) provides another avenue for fabrication of porous materials by building them in a layer-by-layer fashion. Laser powder bed fusion (PBF-LB) is an AM technique, that uses a laser as a heat source to melt thin layers of metal powder in the shape of the desired CAD file. This has broadened the design space for orthopedic implants by allowing the fabrication of porous materials that can tailor the strength and stiffness of metal parts. Ti-6Al-4V (Ti64) is a common metal used in orthopedic implant due to its good biocompatibility and has an elastic modulus of 102 – 110.8 GPa [4,5]. Bone has a wide range of elastic moduli depending on the type of bone but it can range from 0.02 – 28.0 GPa [6,7], which is at least a magnitude smaller than Ti64. This mismatch in mechanical properties of Ti64 and bone is one of the main causes of stress shielding. Lattices, such as FCC or TPMS-Gyroid can be manufactured using AM and used to tailor the stiffness and reduce the elastic modulus, however these structures can be further improved by tailoring them to match the topology of bone as well [7]. The present study explores an alternative method of creating porous structures. By tailoring PBF-LB process parameters, such as hatch spacing and rotation angle, the relative density can be reduced, and unique porous architectures can be formed.

2. Materials and methods

2.1. Laser powder bed fusion process

Gas atomized Ti-6Al-4V powder (AP&C, Canada) with a particle size range of 15 – 45 µm was used. Figure 1 shows an SEM image of the powder. Cylindrical samples with a diameter of 5 mm and a height of 8.7 mm were printed for all sets

of process parameters. Samples were printed on a titanium reduced build volume (RBV) plate of a modulated laser powder bed fusion machine (Renishaw AM400, Renishaw, UK). The machine has a focused beam spot diameter of 70 µm. The layer thickness was kept constant at 30 µm (l_t).

2.2. Experimental design

Dimensionless process mapping was used to determine the set of process parameter combinations (also referred to as recipes) used for this study. Two dimensionless variables, namely E* and v*, were used in a design of experiment to map out process parameters. E* represents the dimensionless heat input and includes a combination of process parameters (such as power (P)) and the material's thermophysical properties (such as laser absorptivity (A) and thermal conductivity (λ), melting point (T_m) and build plate temperature (T_o). v* represents the dimensionless beam velocity, which includes velocity (v), beam spot radius (r_b) and thermal diffusivity (α) [8].

$$E^* = \frac{AP}{2l_t\lambda(T_m - T_o)} \quad \text{(Equation 1)}$$

$$v^* = \frac{vr_b}{\alpha} \quad \text{(Equation 2)}$$

An initial study was conducted with 5 levels of v* and 4 levels of E*, resulting in 20 recipes spanning the conduction, transition and keyhole melting modes in PBF-LB. The range of powers and velocities used were 40.3 – 199.8 W and 0.18 – 1.47 m/s, respectively. One recipe in the conduction melting mode (E* = 20.6, v* = 2.39) was selected for this study to focus on studying the effect of varying hatch spacing and rotation angle, as it resulted in good density. The specifics of the process parameter development are out of scope for the present study. The hatch spacing was varied from 100 – 500 µm in increments of 100 µm. Rotation angles 60º and 67º were applied for all levels of hatch spacing. The process parameters varied for this study are reported in Table 1. Figure 2 shows optical microscopy images of select samples with different hatch spacings and rotation angles.

Table 1. Laser powder bed fusion process parameters and the resulting relative density and sintered powder fraction.

Sample ID	Hatch spacing [µm]	Rotation angle [°]	Relative density (%)	Fraction of sintered powder (%)
1	100	67	99.98	0.00
2	200	67	90.97	6.61
3	300	67	78.91	9.70
4	400	67	72.97	16.52
5	500	67	60.73	11.32
6	100	60	99.98	0.00
7	200	60	88.74	8.13
8	300	60	81.56	19.57
9	400	60	63.37	11.98
10	500	60	50.20	9.66

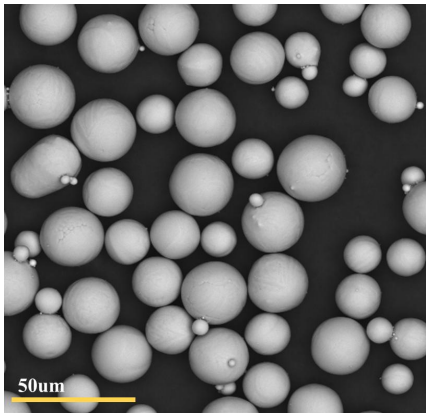

Figure 1. SEM of Ti-6Al-4V powder.

2.3. Characterization methods

The samples were removed from the build plate using a bandsaw. Optical microscopy images were taken with a VHX700 Digital Microscope (Keyence, Japan). To obtain the relative density with high accuracy, XCT was conducted (Xradia 520 Versa, ZEISS, Germany) with a voxel size of 6 µm. Analysis of the XCT data was performed using Dragonfly 3.0 software (Object Research Systems Inc., Canada). Each sample was separated into 3 regions – full solid, "fuzzy" sintered powder, and void. The reported relative density includes the fractions of full solid and the "fuzzy" sintered powder region.

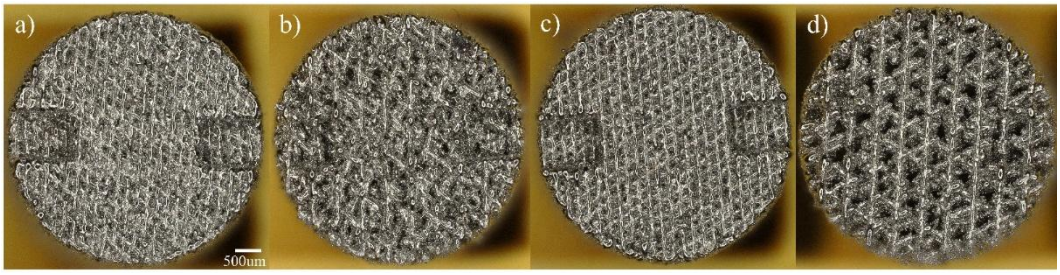

Figure 2. Top-down (XY) view of a) sample 2: hatch spacing 200 µm, rotation angle 67°, b) sample 5: hatch spacing 500 µm, rotation angle 67°, c) sample 7: hatch spacing 200 µm, rotation angle 60°, d) sample 10: hatch spacing 500 µm, rotation angle 60°.

3. Results and discussion

3.1. Effect of hatch spacing on density and pore morphology

The observed trend for both rotation angles is that increasing hatch spacing results in a decrease in density, as anticipated. Table 1 reports the relative density associated with each parameter and the fraction of sintered powder. When looking at the sintered powder region, the volume fraction initially increases with increasing hatch spacing, reaches a maximum value at an intermediary hatch spacing and decreases while the hatch spacing continues to increase. This effect can be seen in both rotation angles; however, the maximum volume fraction occurs at different hatch spacings, visualized in Figure 2. In terms of pore morphology, as the hatch spacing increases, the pore size increases correspondingly. This can be observed in Figure 4, where the pore width increases from Figure 4a to Figure 4e as the hatch spacing increases.

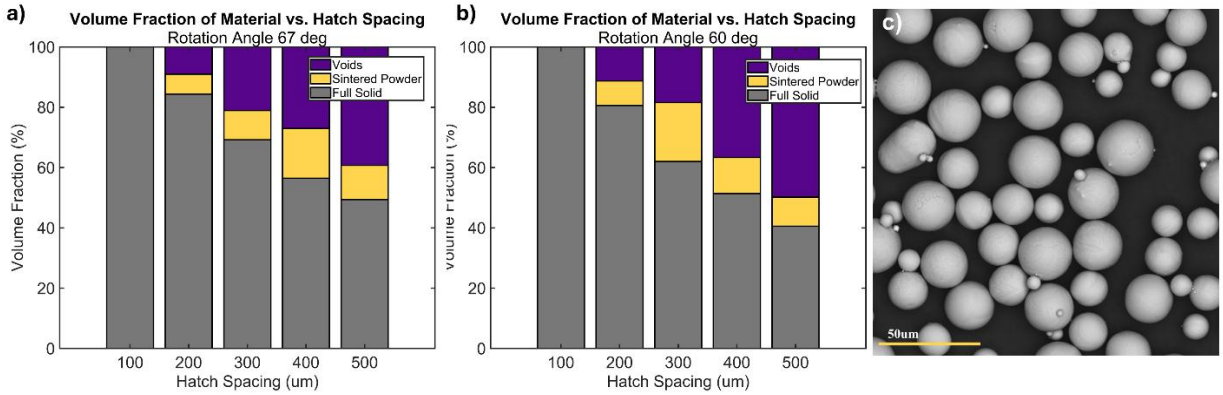

Figure 3. a) Volume fraction of each region at different hatch spacings with a rotation angle of 67°. b) Volume fraction of each region at different hatch spacings with a rotation angle of 60°. c) SEM image of Ti-6Al-4V powder.

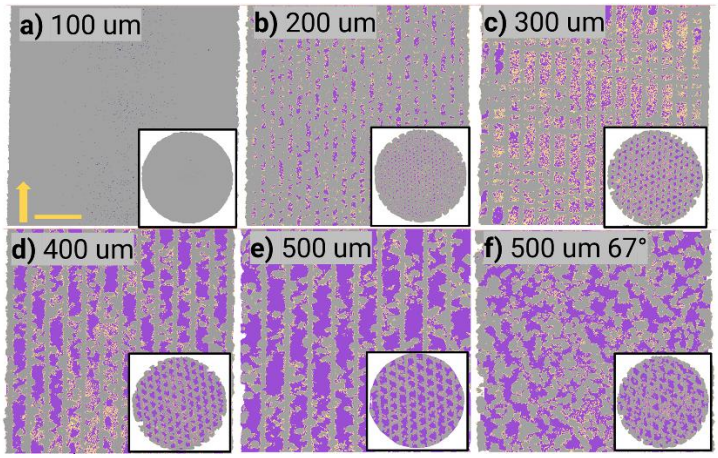

Figure 4. a) – e) 2D cross-section (XZ) of XCT scan of samples 6-10 at hatch spacings 100 – 500 µm with 60° rotation angle, f) sample 5 at hatch spacing of 500 µm with 67° rotation angle. The inset shows the XY view of each sample. Grey is solid region, yellow is sintered powder region and purple is voids. Scale bar is 1 mm, and the arrow indicates build direction.

This decrease in density is due to the lack of overlapping between adjacent melt tracks as the hatch spacing increases. It creates regions that are not melted within the structure and the loose powder can get pulled into melt pools through denudation [9] or get removed from the structure during the de-powdering process. Sintered powder occurs due to loose powder that is near the outer region of the melt pool, where the temperature is not high enough to melt the powder but enough to adhere it to the weld track. This creates a different surface texture compared to fully melted solid. The trend of decreasing density with increasing hatch spacing is consistent with a previous study conducted by Sardarian et al. [10] who explored hatch spacings of 61 – 129 µm.

3.2. Effect of rotation angle on density and pore morphology

At low densities, rotation angle has an impact on density. When comparing the density of samples 5 and 10, both have hatch spacing of 500 µm, the 67º sample has a higher relative density of 60.73% and the 60º sample has a relative density of 50.20%. This effect can also be visually observed in the Figure 2b and Figure 2d, where in 2d, there is more void space and distinct regions that are not scanned by the laser. This trend is consistent at all hatch spacings tested in this study. In terms of pore morphology, 67º rotation angle resulted in a more random or stochastic distribution of pores.

Figure 4f shows the random pore morphology of the pores at a 500 µm hatch spacing. Comparing this with a 60º rotation angle, there is a repeated pattern to the pores such that they are more columnar, which is seen in Figures 4b to Figure 4e.

A 67° rotation angle is a common angle used in PBF-LB as it results in a more random scan pattern to reduce the number of defects or keep a random distribution of defects caused by rotation angle. With a 67° rotation angle, more of the cross section gets scanned, resulting in a higher density. At a 60° rotation angle, only certain regions of the cross section get scanned repeatedly, therefore decreasing the overall density. Studies on the effect of rotation angle on density of low-density samples are rare. Zhou et al. [11] studied the effect of 0°, 15°, 30°, 45°, 67° and 90° rotation angles on density with a goal of printing high density AlSi10Mg and concluded that rotation angle has no effect on density. However, the results from this study show that when printing low-density samples, rotation angle affects density. In terms of pore morphology, Vanmunster et al. [12] explored printing low-density Ti-6Al-4V structures with a 90° rotation angle and hatch spacing of 167 µm and observed rectangular columnar pores with density of 84%, similar to what is observed in the present study.

4. Conclusion

In this work, the effect of hatch spacing and rotation angle on density and pore morphology have been investigated. It was shown that hatch spacing has a larger impact on density, with increasing hatch spacing resulting in decreasing density. Rotation angle also influences the density when targeting low density samples and has a large impact on pore morphology. The achieved densities ranged from 50.20 – 99.98%, depending on the combination of hatch spacing and rotation angle. Two types of pore morphologies were obtained by changing the rotation angle, with the 67° resulting in a stochastic distribution and shape, and 60° resulting in a structured distribution and shape. Findings from this work can be incorporated in future design of orthopedic implants as an alternative method of reducing stress shielding and tailoring mechanical response. Future studies should explore the effect these parameters have on mechanical performance as well as biological performance based on the different surface textures created.

5. Acknowledgments

The authors would like to acknowledge the funding support from FedDev Ontario and the help of Jerry Ratthapakee, Edward Yang and Sebastian Soo for their help with deployment and characterization of build and the motivation and support of the MSAM Group at the University of Waterloo.

6. Conflicts of interest

The authors declare that they have no conflicts of interest that could influence the research conducted in this paper.

7. References

[1] Vacanti JP, Langer R. Tissue engineering: the design and fabrication of living replacement devices for surgical reconstruction and transplantation. The Lancet. 1999 Jul 1;354:S32–4.
[2] Widmer AF. New Developments in Diagnosis and Treatment of Infection in Orthopedic Implants. Clin Infect Dis. 2001 Sep 1;33(Supplement_2):S94–106.
[3] Naghavi SA, Lin C, Sun C, Tamaddon M, Basiouny M, Garcia-Souto P, et al. Stress Shielding and Bone Resorption of Press-Fit Polyether–Ether–Ketone (PEEK) Hip Prosthesis: A Sawbone Model Study. Polymers. 2022 Oct 29;14(21):4600.
[4] Bittredge O, Hassanin H, El-Sayed MA, Eldessouky HM, Alsaleh NA, Alrasheedi NH, et al. Fabrication and Optimisation of Ti-6Al-4V Lattice-Structured Total Shoulder Implants Using Laser Additive Manufacturing. Materials. 2022 Jan;15(9):3095.
[5] He Z, He H, Lou J, Li Y, Li D, Chen Y, et al. Fabrication, Structure and Mechanical and Ultrasonic Properties of Medical Ti6Al4V Alloys Part I: Microstructure and Mechanical Properties of Ti6Al4V Alloys Suitable for Ultrasonic Scalpel. Materials. 2020 Jan 19;13(2):478.
[6] Barba D, Alabort E, Reed RC. Synthetic bone: Design by additive manufacturing. Acta Biomater. 2019 Oct;97:637–56.
[7] McGregor M, Patel S, McLachlin S, Mihaela Vlasea. Architectural bone parameters and the relationship to titanium lattice design for powder bed fusion additive manufacturing. Addit Manuf. 2021 Nov;47:102273.
[8] Patel S, Vlasea M. Melting modes in laser powder bed fusion. Materialia. 2020 Mar;9:100591.
[9] Matthews MJ, Guss G, Khairallah SA, Rubenchik AM, Depond PJ, King WE. Denudation of metal powder layers in laser powder bed fusion processes. Acta Mater. 2016 Aug;114:33–42.
[10] Sardarian S, Dehgahi S, Wei F, Secanell M, Qureshi AJ. Structured porous 17-PH stainless steel layer fabrication through laser powder bed fusion. Int J Sustain Eng. 2024 Dec 31;17(1):1–16.
[11] Zhou L, Yang H, Hyer H. Controlling mechanical properties of laser powder bed fused AlSi10Mg through manipulation of laser scan rotation. Materialia. 2025 Mar;39:102340.
[12] Vanmunster L, D'Haeyer C, Coucke P, Braem A, Van Hooreweder B. Mechanical behavior of Ti6Al4V produced by laser powder bed fusion with engineered open porosity for dental applications. J Mech Behav Biomed Mater. 2022 Feb 1;126:104974.